Supplementary Material (ESI) for Organic & Biomolecular Chemistry

SUPPORTING INFORMATION

for

Kinetic studies of retinol addition radicals

Ali El-Agamey,[a,b,c] Shunichi Fukuzumi,*[a,d] K. Razi Naqvi,[e] and David J McGarvey[b]

[a]Department of Material and Life Science, Graduate School of Engineering, Osaka University, Suita, Osaka 565-0871, Japan; [b]School of Physical and Geographical Sciences, Keele University, Keele, Staffordshire, ST5 5BG, UK; [c]Chemistry Department, Faculty of Science, Mansoura University, New Damietta, Damietta, Egypt; [d]Department of Bioinspired Science, Ewha Womans University, Seoul 120-750, Korea; [e]Department of Physics, Norwegian University of Science and Technology (NTNU), N-7491, Trondheim, Norway.

*Corresponding authors: Ali El-Agamey (Osaka University); Shunichi Fukuzumi (Osaka University)

E-mails: a_el_agamey@yahoo.co.uk; fukuzumi@chem.eng.osaka-u.ac.jp Tel. No.: +81-0668797369; Fax No.: +81-0668797370

Contents

Fig. S8 Plots of pseudo-first order rate constants (k_{obs}) for formation of PhS-retinol$^{\bullet}$, 4-PyrS-retinol$^{\bullet}$ or 2-PyrS-retinol$^{\bullet}$ at 380 nm, from the reaction of retinol with phenyl disulfide, 4, 4`-dipyridyl disulfide or 2, 2`-dipyridyl disulfide, respectively in air-saturated methanol versus the concentration of retinol (laser energy ~4.0 mJ).

Fig. S9 Kinetic absorption profiles for the formation of 4-PyrS-retinol$^{\bullet}$ at 380 nm at various retinol concentrations formed following 266 nm laser photolysis (laser energy ~4 mJ) of 4, 4`-dipyridyl disulfide (~2.0×10^{-4} M) in the presence of retinol in air-saturated methanol.

Fig. S10 Kinetic absorption profiles for the formation of 2-PyrS-retinol$^{\bullet}$ at 380 nm at various retinol concentrations formed following 266 nm laser photolysis (laser energy ~4 mJ) of 2, 2`-dipyridyl disulfide (~3.0×10^{-4} M) in the presence of retinol in air-saturated methanol.

Fig. S11 Kinetic absorption profiles for the formation of PhS-retinol$^{\bullet}$ at 380 nm at various retinol concentrations formed following 266 nm laser photolysis (laser energy ~4 mJ) of phenyl disulfide (~6.0×10^{-4} M) in the presence of retinol in air-saturated methanol.

Fig. S12 Arrhenius plot for the slow growth (at 380 nm) generated from the reaction of 4-PyrS$^{\bullet}$ (4,4`-dipyridyl disulfide ~2×10^{-4} M) and retinol (~8.0×10^{-5} M), in argon-saturated methanol (laser energy ~4 mJ).

Fig. S13 Transient spectra of 4-PyrS-retinol$^{\bullet}$ obtained following 266 nm laser photolysis of 4, 4`-dipyridyl disulfide (~2.0×10^{-4} M) in the presence of retinol (~4.0×10^{-5} M) in air-saturated methanol at 334 K (laser energy ~4 mJ). The inset shows a kinetic absorption profile of 4-PyrS-retinol$^{\bullet}$ at 380 nm.

Fig. S14 Eyring plots for the slow growth (at 380 nm) generated from the reaction of 4-PyrS$^{\bullet}$ or 2-PyrS$^{\bullet}$ with retinol (~8.0×10^{-5} M), in argon-saturated methanol (laser energy ~4 mJ).

Fig. S15 Transient profiles, at 380 nm, for 4-PyrS-retinol$^{\bullet}$ and 4-PyrS$^{\bullet}$ in argon-saturated methanol at 334 K (laser energy ~4 mJ).

Fig. S16 Transient profiles, at 380 nm, for 2-PyrS-retinol$^{\bullet}$ and 2-PyrS$^{\bullet}$ in argon-saturated methanol at 334 K (laser energy ~4 mJ).

Fig. S17 Transient profile of PhS-retinol$^{\bullet}$, at 380 nm, following 266 nm laser photolysis (laser energy ~4 mJ) of phenyl disulfide (~6×10^{-4} M) in the presence of retinol (~9.0×10^{-5} M), in argon-saturated methanol at 333 K.

Fig. S18 Normalized kinetic absorption profiles for the decay of 4-PyrS-retinol$^{\bullet}$ at 380 nm in methanol at various oxygen concentrations (5, 21, 50 and 100%) formed following 266 nm laser photolysis (laser energy ~4 mJ) of 4, 4`-dipyridyl disulfide (~2×10^{-4} M) in the presence of retinol (~8.0×10^{-5} M). The inset shows plots of pseudo-first order rate constants (k_{obs}) for the fast and slow decay of 4-PyrS-retinol$^{\bullet}$, at 380 nm, versus the oxygen concentration.

Fig. S19 The influence of temperature on the normalized transient profiles, at 380 nm, of 2-PyrS-retinol$^{\bullet}$ following 266 nm laser photolysis (laser energy ~4 mJ) of 2, 2`-dipyridyl disulfide (~3.0×10^{-4} M) in the presence of retinol (~8×10^{-5} M), in air-saturated methanol.

Fig. S20 Plots of pseudo-first order rate constants (k_{obs}) for the fast and slow decay of PhS-retinol$^{\bullet}$ at 380 nm, generated following 266 nm laser photolysis of phenyl disulfide (~6×10^{-4} M) with retinol (~9.0×10^{-5} M) in methanol, versus the oxygen concentration (laser energy ~4 mJ). The inset shows normalized kinetic absorption profiles for the decay of PhS-retinol$^{\bullet}$, at 380 nm, at various oxygen concentrations (1, 5, 21, 50, 100% and argon).

Fig. S21 The influence of temperature on the normalized transient profiles, at 380 nm, of PhS-retinol$^{\bullet}$ following 266 nm laser photolysis (laser energy ~4 mJ) of phenyl disulfide (~6×10^{-4} M) in the presence of retinol (~9.0×10^{-5} M), in air-saturated methanol.

Table S1: Values of k_{obs} for the slow absorption rise at 380 nm following 266 nm LFP (laser energy ~4 mJ) of 4, 4`-dipyridyl disulfide (~2×10^{-4} M) in the presence of retinol (~8.0×10^{-5} M), in argon-saturated methanol at different temperatures.

Table S2: Values of k_{obs} for the slow absorption rise at 380 nm following 266 nm LFP (laser energy ~4 mJ) of 2, 2`-dipyridyl disulfide (~3.0×10^{-4} M) in the presence of retinol (~8.0×10^{-5} M), in argon-saturated methanol at different temperatures.

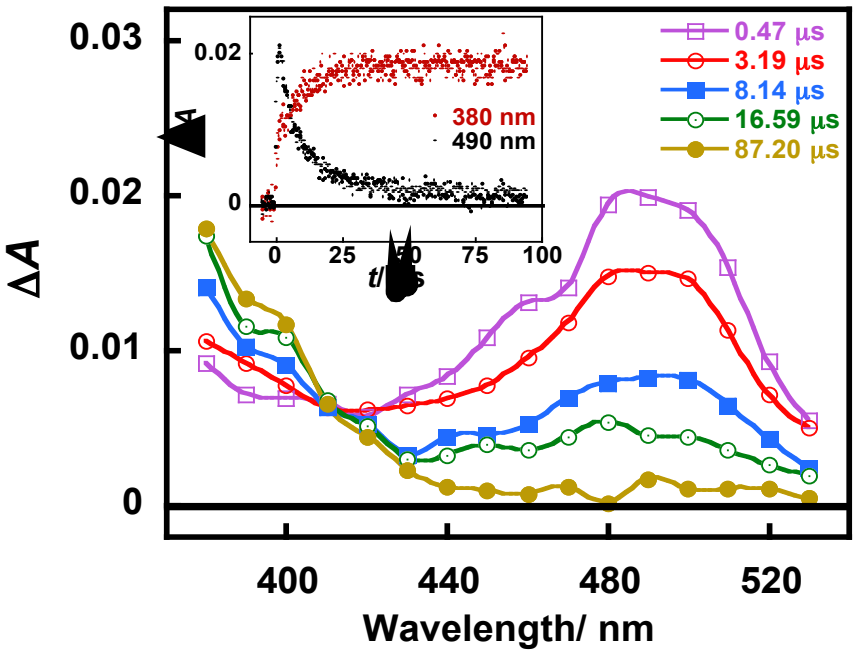

Fig. S1 Transient spectra of 2-PyrS$^{\bullet}$ obtained following 266 nm laser photolysis of 2, 2`-dipyridyl disulfide (~3.0 × 10^{-4} M) in air-saturated methanol (laser energy ~7 mJ). The inset shows the transient profiles at 380 and 490 nm.

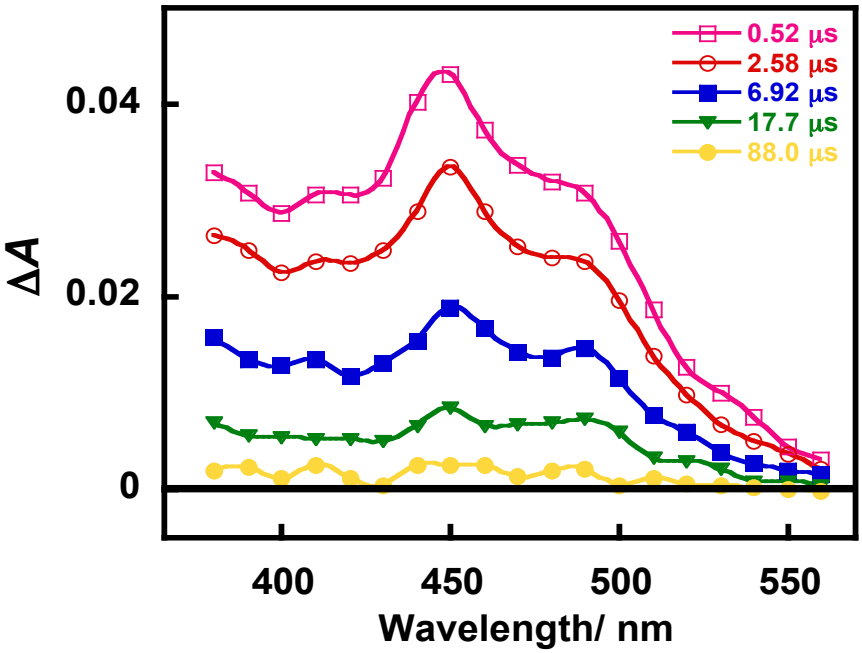

Fig. S2 Transient absorption spectra obtained following LFP (266 nm) of phenyl disulfide (~6 × 10^{-4} M) in air-saturated methanol (laser energy ~10 mJ).

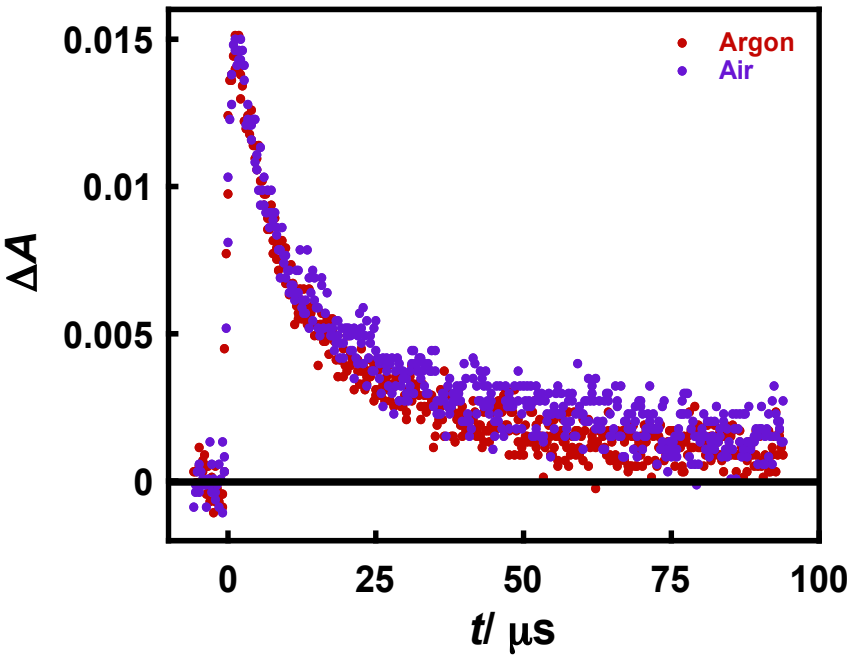

Fig. S3 Normalized kinetic absorption profiles for the decay of $PhS^{\bullet}$ at 450 nm in air- and argon-saturated methanol (laser energy ~4 mJ).

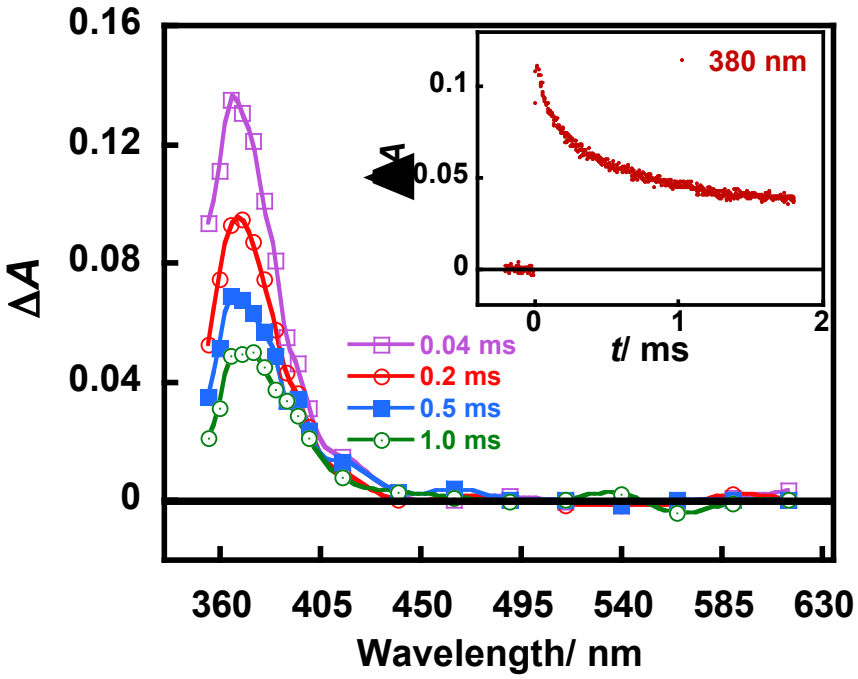

Fig. S4 Transient spectra of 2-PyrS-retinol$^{\bullet}$ obtained following 266 nm laser photolysis of 2, 2`-dipyridyl disulfide (~3.0×10^{-4} M) in the presence of retinol (~5.0×10^{-5} M) in air-saturated methanol at room temperature (laser energy ~4 mJ). The inset shows a kinetic absorption profile for the decay of 2-PyrS-retinol$^{\bullet}$ at 380 nm.

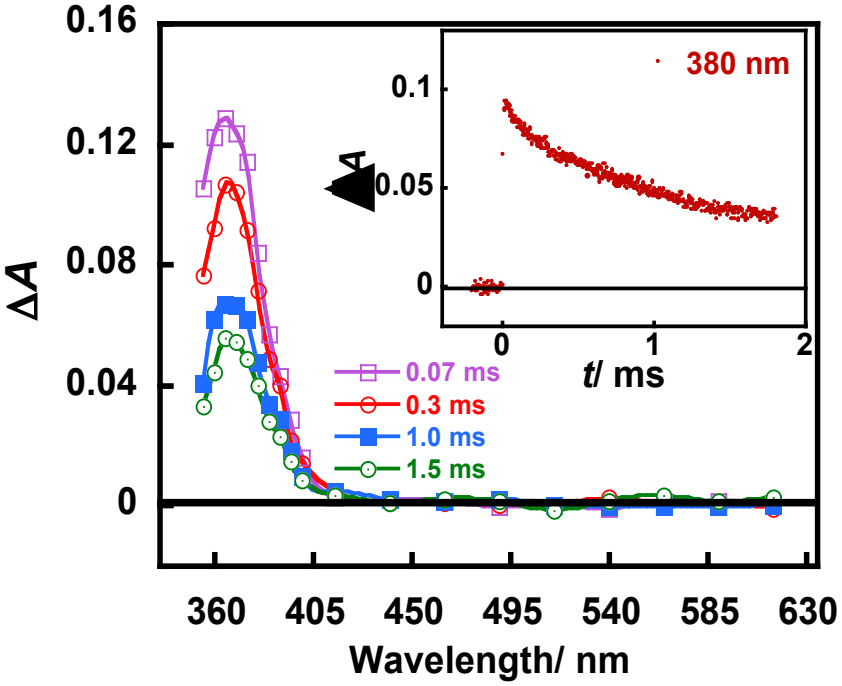

Fig. S5 Transient spectra of PhS-retinol$^{\bullet}$ obtained following 266 nm laser photolysis of phenyl disulfide (~6 × 10^{-4} M) in the presence of retinol (~5.0 × 10^{-5} M) in air-saturated methanol at room temperature (laser energy ~4 mJ). The inset shows a kinetic absorption profile for the decay of PhS-retinol$^{\bullet}$ at 380 nm.

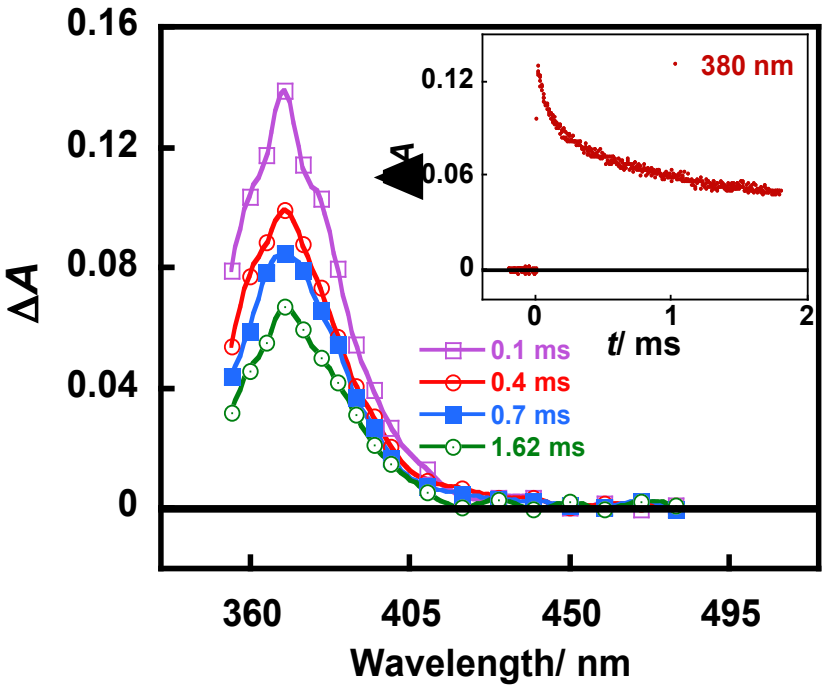

Fig. S6 Transient spectra of 4-PyrS-retinol$^{\bullet}$ obtained following 266 nm laser photolysis of 4, 4`-dipyridyl disulfide (~1.0×10^{-4} M) in the presence of retinol (~4.0×10^{-5} M) in air-saturated cyclohexane at room temperature (laser energy ~4 mJ). The inset shows a kinetic absorption profile for the decay of 4-PyrS-retinol$^{\bullet}$ at 380 nm.

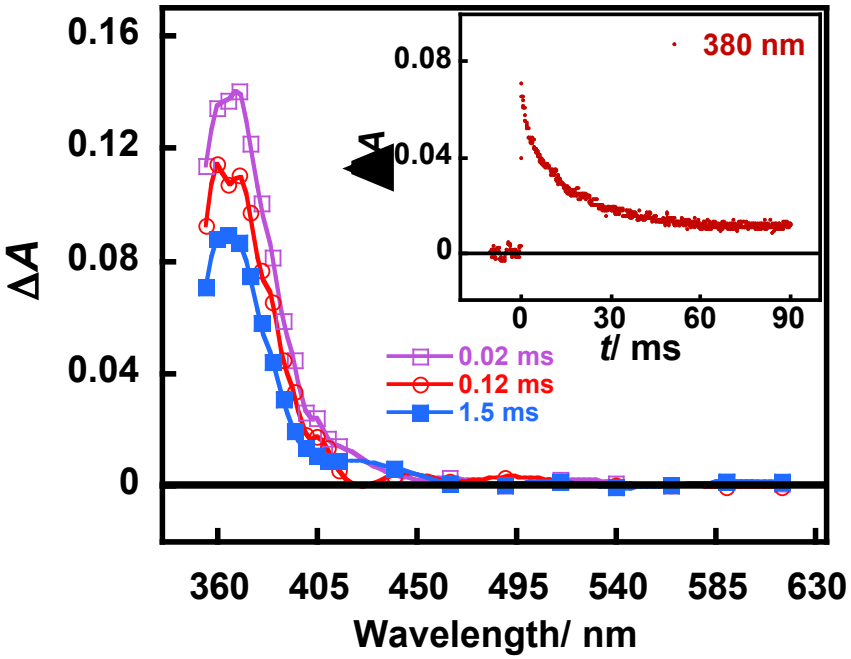

Fig. S7 Transient spectra of 4-PyrS-retinol$^{\bullet}$ obtained following 266 nm laser photolysis of 4, 4`-dipyridyl disulfide (~2.0×10^{-4} M) in the presence of retinol (~4.0×10^{-5} M) in argon-saturated methanol at room temperature (laser energy ~4 mJ). The inset shows a kinetic absorption profile for the decay of 4-PyrS-retinol$^{\bullet}$ at 380 nm.

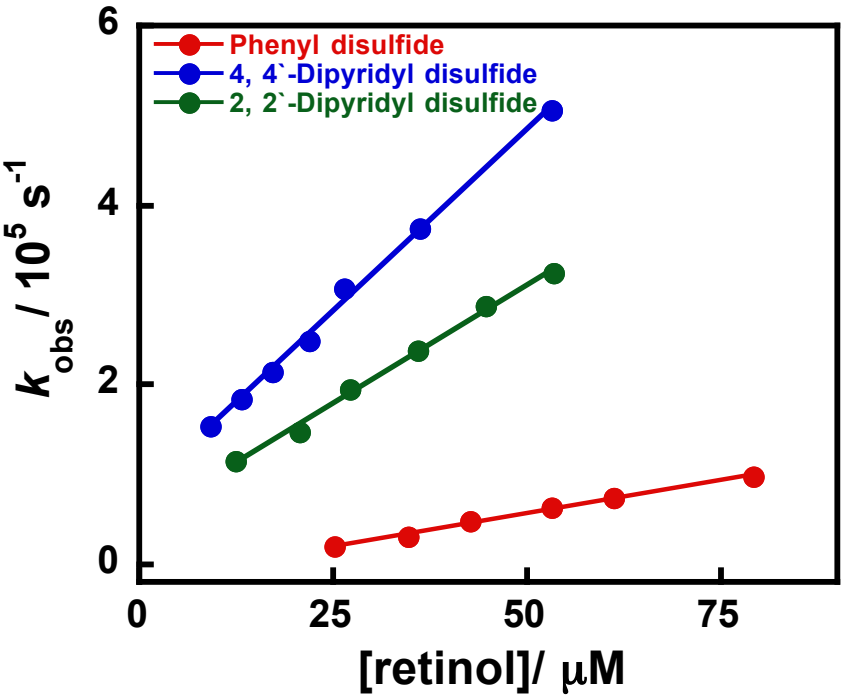

Fig. S8 Plots of pseudo-first order rate constants (k_{obs}) for formation of PhS-retinol$^{\bullet}$, 4-PyrS-retinol$^{\bullet}$ or 2-PyrS-retinol$^{\bullet}$ at 380 nm, from the reaction of retinol with phenyl disulfide, 4, 4`-dipyridyl disulfide or 2, 2`-dipyridyl disulfide, respectively in air-saturated methanol versus the concentration of retinol (laser energy ~4.0 mJ).

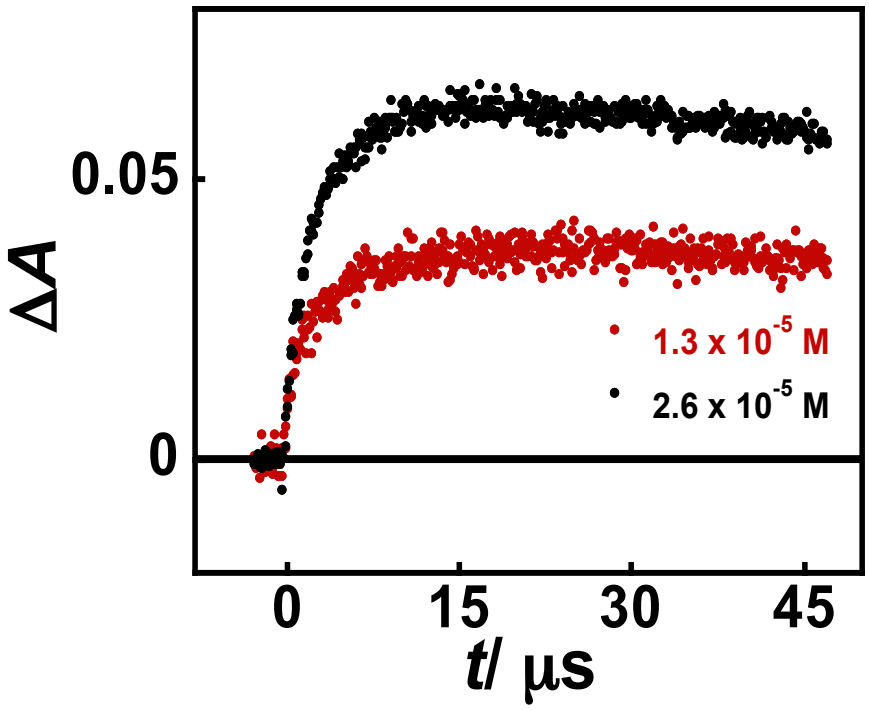

Fig. S9 Kinetic absorption profiles for the formation of 4-PyrS-retinol$^{\bullet}$ at 380 nm at various retinol concentrations formed following 266 nm laser photolysis (laser energy ~4 mJ) of 4, 4`-dipyridyl disulfide (~2.0 × 10^{-4} M) in the presence of retinol in air-saturated methanol.

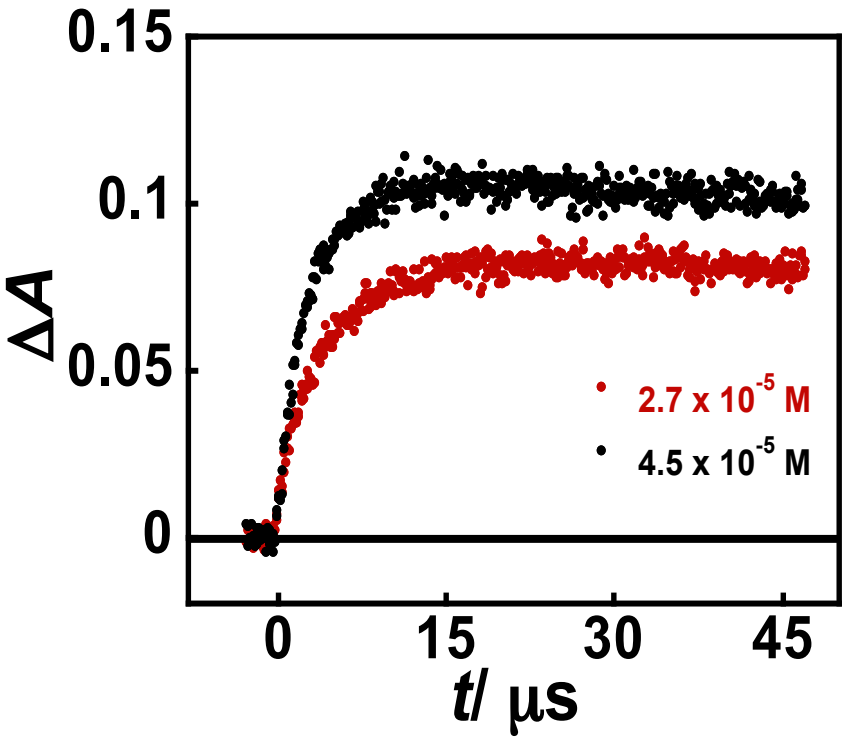

Fig. S10 Kinetic absorption profiles for the formation of 2-PyrS-retinol$^{\bullet}$ at 380 nm at various retinol concentrations formed following 266 nm laser photolysis (laser energy ~4 mJ) of 2, 2`-dipyridyl disulfide (~3.0×10^{-4} M) in the presence of retinol in air-saturated methanol.

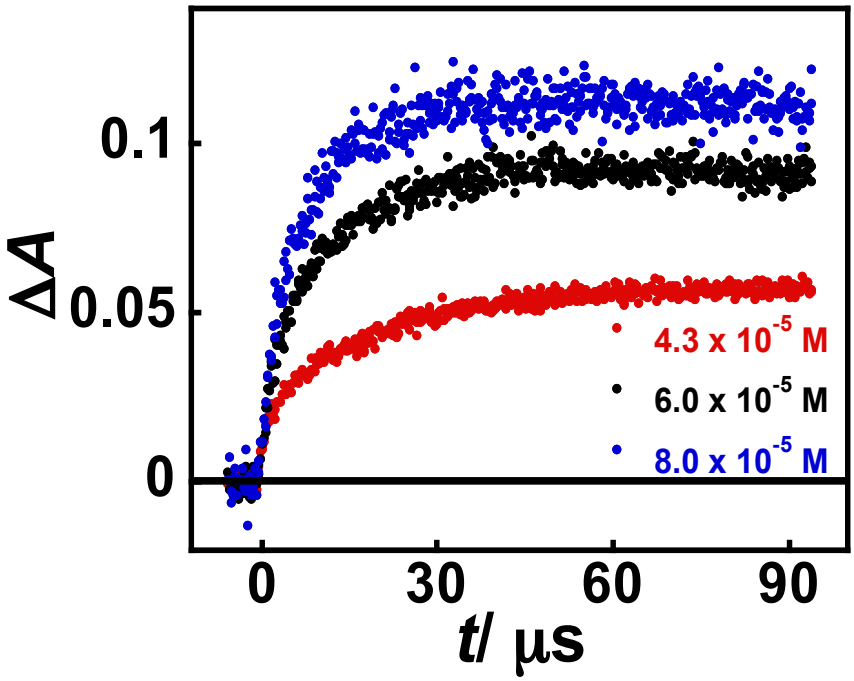

Fig. S11 Kinetic absorption profiles for the formation of PhS-retinol$^{\bullet}$ at 380 nm at various retinol concentrations formed following 266 nm laser photolysis (laser energy ~4 mJ) of phenyl disulfide (~6.0×10^{-4} M) in the presence of retinol in air-saturated methanol.

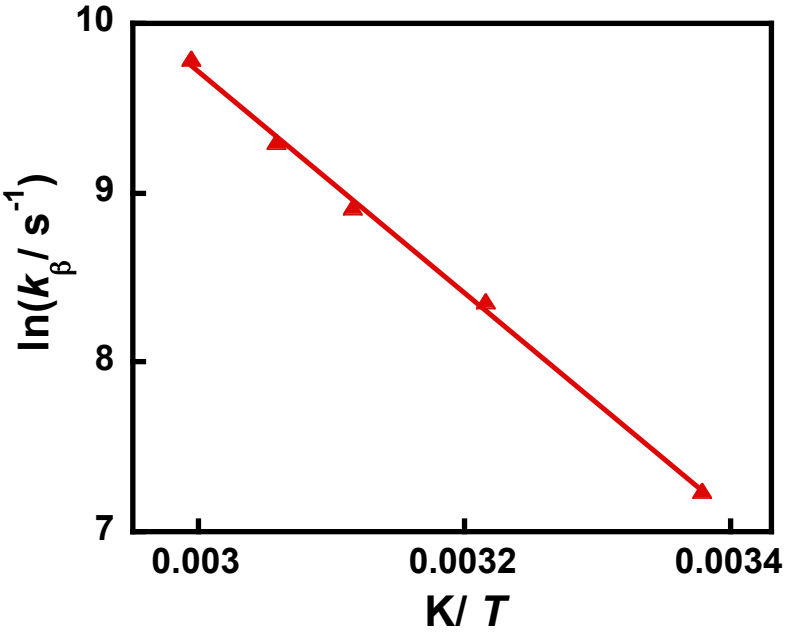

Fig. S12 Arrhenius plot for the slow growth (at 380 nm) generated from the reaction of 4-PyrS$^{\bullet}$ (4,4`-dipyridyl disulfide ~2 × 10^{-4} M) and retinol (~8.0 × 10^{-5} M), in argon-saturated methanol (laser energy ~4 mJ).

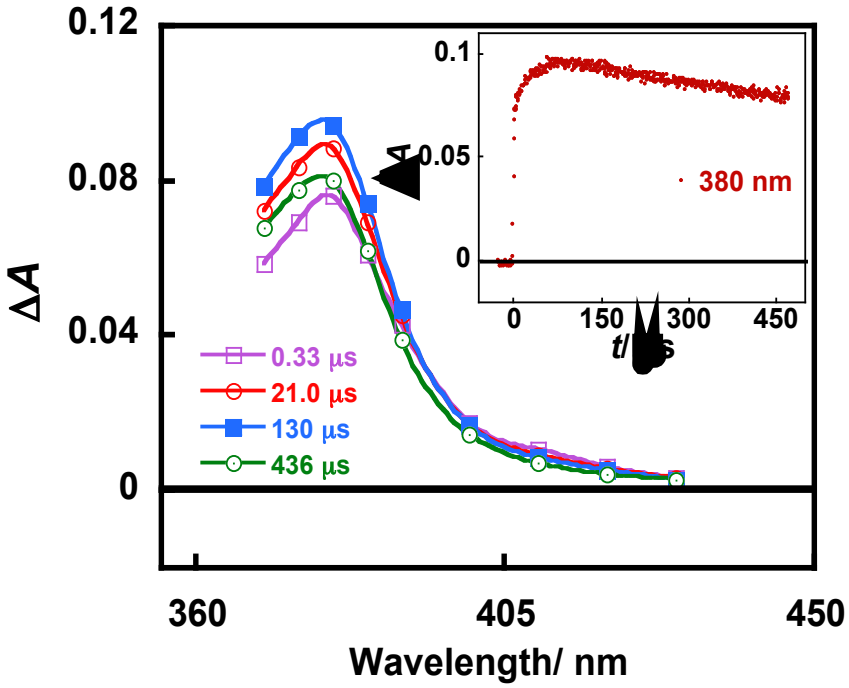

Fig. S13 Transient spectra of 4-PyrS-retinol$^{\bullet}$ obtained following 266 nm laser photolysis of 4, 4`-dipyridyl disulfide (~2.0×10^{-4} M) in the presence of retinol (~4.0×10^{-5} M) in air-saturated methanol at 334 K (laser energy ~4 mJ). The inset shows a kinetic absorption profile of 4-PyrS-retinol$^{\bullet}$ at 380 nm.

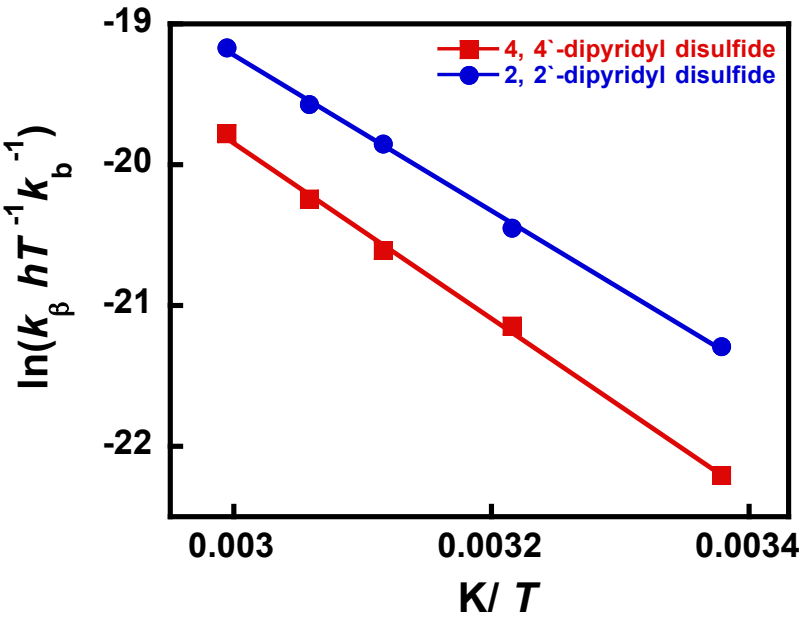

Fig. S14 Eyring plots for the slow growth (at 380 nm) generated from the reaction of 4-PyrS$^{\bullet}$ or 2-PyrS$^{\bullet}$ with retinol (~8.0 × 10^{-5} M), in argon-saturated methanol (laser energy ~4 mJ).

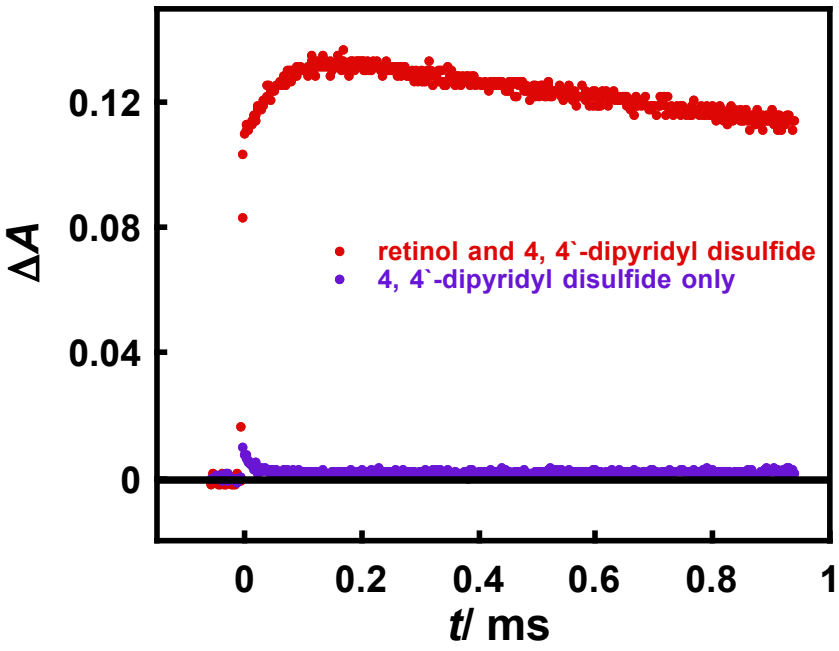

Fig. S15 Transient profiles, at 380 nm, for 4-PyrS-retinol$^{\bullet}$ and 4-PyrS$^{\bullet}$ in argon-saturated methanol at 334 K (laser energy ~4 mJ).

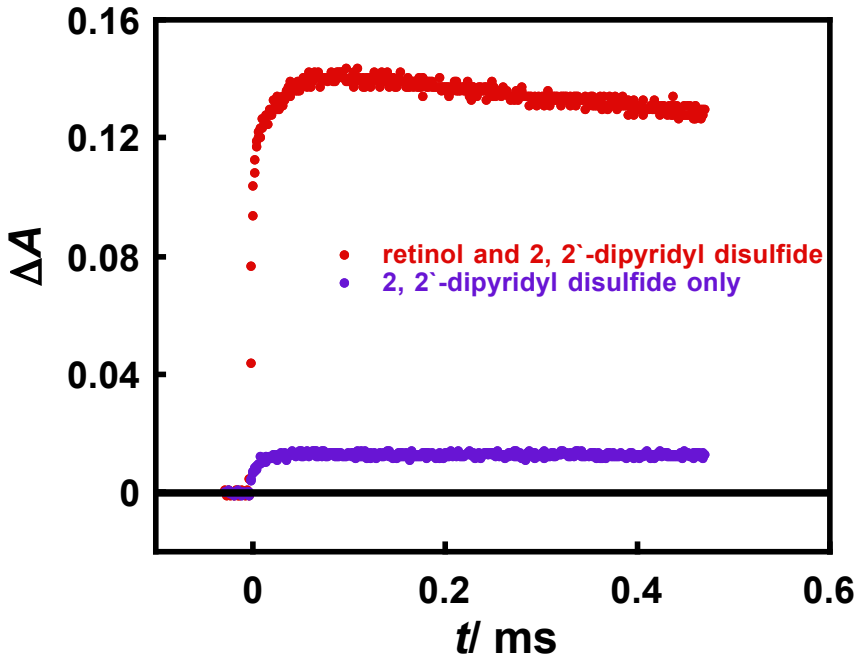

Fig. S16 Transient profiles, at 380 nm, for 2-PyrS-retinol$^{\bullet}$ and 2-PyrS$^{\bullet}$ in argon-saturated methanol at 334 K (laser energy ~4 mJ).

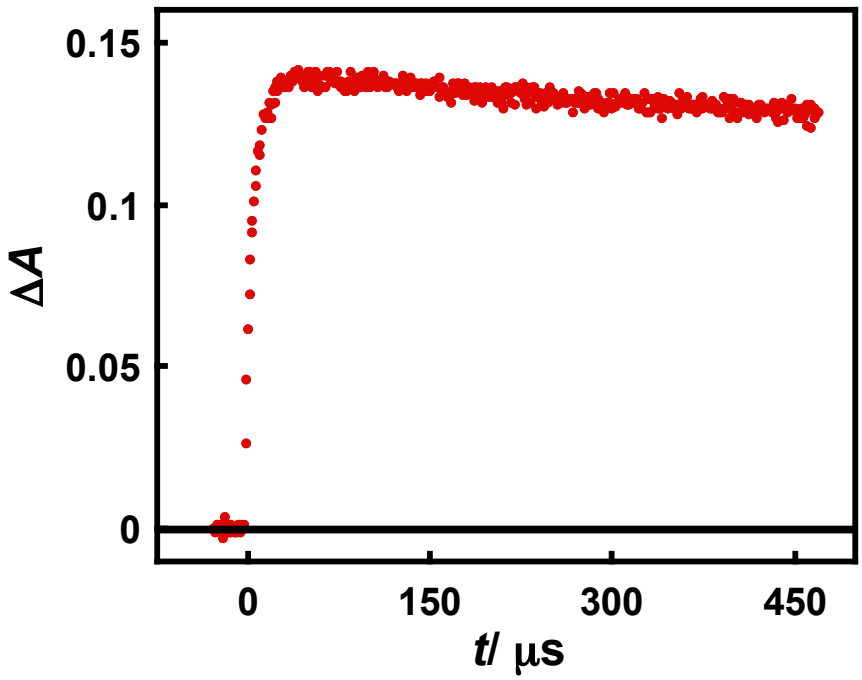

Fig. S17 Transient profile of PhS-retinol$^{\bullet}$, at 380 nm, following 266 nm laser photolysis (laser energy ~4 mJ) of phenyl disulfide (~6 × 10^{-4} M) in the presence of retinol (~9.0 × 10^{-5} M), in argon-saturated methanol at 333 K.

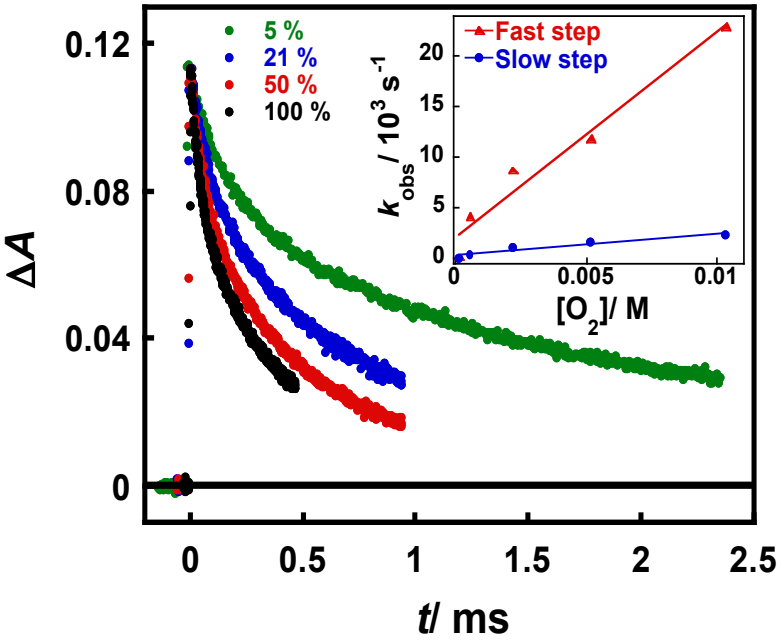

Fig. S18 Normalized kinetic absorption profiles for the decay of 4-PyrS-retinol$^{\bullet}$ at 380 nm in methanol at various oxygen concentrations (5, 21, 50 and 100%) formed following 266 nm laser photolysis (laser energy ~4 mJ) of 4, 4`-dipyridyl disulfide (~2×10^{-4} M) in the presence of retinol (~8.0×10^{-5} M). The inset shows plots of pseudo-first order rate constants (k_{obs}) for the fast and slow decay of 4-PyrS-retinol$^{\bullet}$, at 380 nm, versus the oxygen concentration.

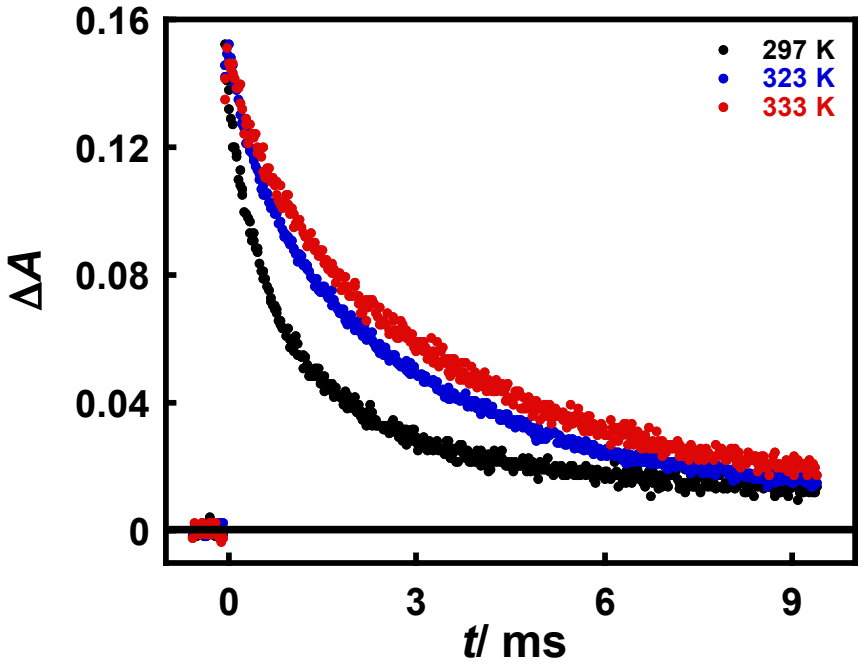

Fig. S19 The influence of temperature on the normalized transient profiles, at 380 nm, of 2-PyrS-retinol$^{\bullet}$ following 266 nm laser photolysis (laser energy ~4 mJ) of 2, 2`-dipyridyl disulfide (~3.0 × 10^{-4} M) in the presence of retinol (~8 × 10^{-5} M), in air-saturated methanol.

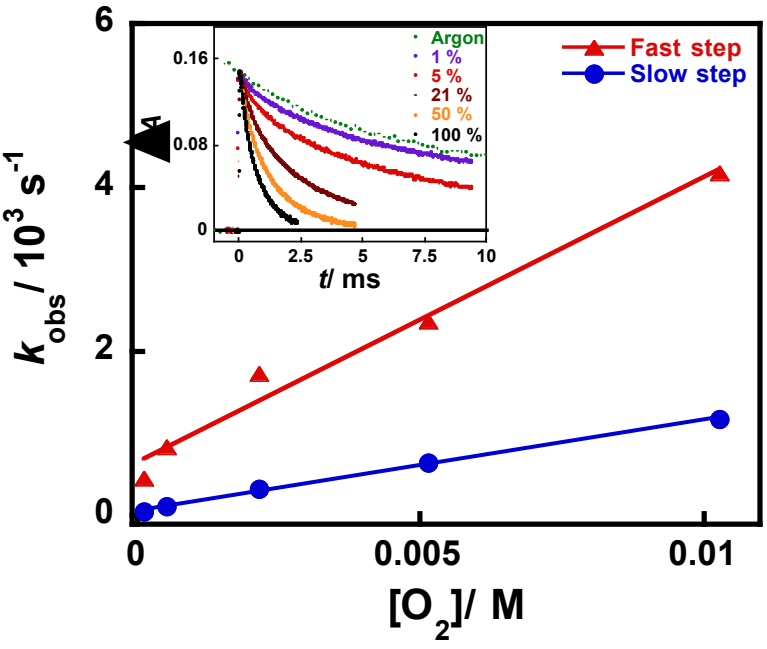

Fig. S20 Plots of pseudo-first order rate constants (k_{obs}) for the fast and slow decay of PhS-retinol$^{\bullet}$ at 380 nm, generated following 266 nm laser photolysis of phenyl disulfide (~6×10^{-4} M) with retinol (~9.0×10^{-5} M) in methanol, versus the oxygen concentration (laser energy ~4 mJ). The inset shows normalized kinetic absorption profiles for the decay of PhS-retinol$^{\bullet}$, at 380 nm, at various oxygen concentrations (1, 5, 21, 50, 100% and argon).

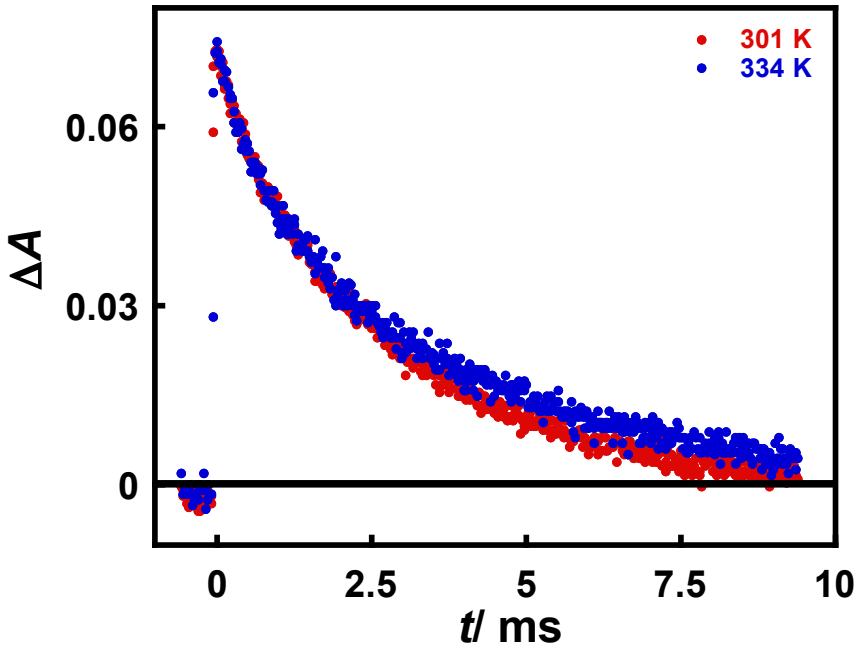

Fig. S21 The influence of temperature on the normalized transient profiles, at 380 nm, of PhS-retinol$^{\bullet}$ following 266 nm laser photolysis (laser energy ~4 mJ) of phenyl disulfide (~6×10^{-4} M) in the presence of retinol (~9.0×10^{-5} M), in air-saturated methanol.

Table S1: Values of k_{obs} for the slow absorption rise at 380 nm following 266 nm LFP (laser energy ~4 mJ) of 4, 4`-dipyridyl disulfide (~2×10^{-4} M) in the presence of retinol (~8.0×10^{-5} M), in argon-saturated methanol at different temperatures.

T/K	k_{obs} for the slow absorption rise/ s^{-1}
334	1.78×10^4
327	1.10×10^4
321	7.45×10^3
311	4.25×10^3
296	1.39×10^3

Table S2: Values of k_{obs} for the slow absorption rise at 380 nm following 266 nm LFP (laser energy ~4 mJ) of 2, 2`-dipyridyl disulfide (~3.0×10^{-4} M) in the presence of retinol (~8.0×10^{-5} M), in argon-saturated methanol at different temperatures.

T/K	k_{obs} for the slow absorption rise/ s^{-1}
334	3.29×10^4
327	2.14×10^4
321	1.60×10^4
311	8.55×10^3
296	3.48×10^3